Free transverse vibration analysis of laminated composite beams with arbitrary number of concentrated masses

Ahmad Reza Ghasemi[1]*, Mohammad Heidari-Rarani[2], Bijan Heidari-Sheibani[1], Ali Tabatabaeian[3]

[1] *Composite and Nanocomposite Research Laboratory, Faculty of Mechanical Engineering, University of Kashan, Kashan, Iran*

[2] *Department of Mechanical Engineering, Faculty of Engineering, University of Isfahan, Isfahan, Iran*

[3] *School of Engineering, University of Glasgow, Glasgow, UK.*

Abstract

In this study, a new closed-form solution for transverse free vibration analysis of laminated composite beams (LCBs) with arbitrary number of concentrated masses is developed. The LCB is modeled based on the Euler-Bernoulli beam theory and concentrated masses are simulated considering Dirac delta function. Obtained governing equations are, then, solved semi-analytically while the frequency equation and mode shapes are extracted for two different boundary conditions, i.e., clamped-free and simply-supported. In order to verify the closed-form solution, the represented model is simplified for a beam without concentrated mass and outcomes are compared with available results in the literature. Finally, the effects of mass as well as location and number of concentrated masses on the free vibration response of the beam are investigated in detail. The results highlight that with increasing the value of point masses, the natural frequencies decrease. Also, it was revealed that the number of point masses influences on the vibration of cantilever beam more than the simply-supported one. These outcomes would practically be used to minimize detrimental effects of vibrational noises, leading to increase of the structural components' lifetime.

Keywords: Free Transverse Vibration, Laminated Composite Beams (LCBs), Concentrated Mass, Exact Solution

---

* Corresponding author: Ahmad Reza Ghasemi, E-mail address: ghasemi@kashanu.ac.ir

1. Introduction

The world of manufacturing engineering is constantly evolving while striving to deal with a number of challenges, such as transverse vibrations due to geometrical imperfections or inaccurate assembly of machine parts. Similarly, detrimental effects associated with physical discontinuities, namely 'concentrated masses', 'presence of cracks and 'presence of ledge on structures' have always been among the primary concerns of researchers in vibrational sciences. An efficient method to mathematically model such mechanical components as gears, chains and couplings is to simulate them as a concentrated mass through the longitudinal axis of a beam or a shaft. This can be particularly seen in aerospace sciences, where the composite wing of an airplane is considered as a beam with concentrated mass.

. Several researches have been conducted regarding free vibration analysis of laminated composite beams related to the concept of "concentrated mass". Banerjee [1] did research on the natural frequencies and mode shapes of a cantilever layered symmetric beams. Ghayesh et al. [2] studied the thermo-mechanical free vibrations of a simply supported with concentrated mass. Yang and Oyadiji [3] investigated the effects of delamination in LCBs due to concentrated mass loading with respect to modal frequency variations. The vibration and stability of rectangular plates in contact with fluid [4-5], vibration of elliptical and circular plates on an elastic foundation [6-7], laminated composite cylinder [8] and free vibration of Euler and Timoshenko LCBs based on finite strain displacement [9-11] have presented in the past researches.

Free vibrations of the non-uniform axially Euler–Bernoulli beam with mass center of the tip body studied by Nikolic [12]. The free vibration analysis of laminated composite shells with cutouts and concentrated mass investigated by Chaubey et al. [13]. In recent years, the wave transmission using prismatic beams with concentrated gradient masses [14], bending vibration generated by tapping cross section with additional mass [15], twist of composite blade with moving mass [16], transverse vibrations of nanobeam with a single point mass [17] and dynamic stability of spinning thin-walled composite beams carrying rigid bodies [18] are presented.

Above literature review arguably highlighted that in spite of numerous researches being performed regarding free vibration response of composite beams, vibrational analysis of composite beams with arbitrary number of point masses has not been carried out in structural engineering community. This research, therefore, aims to focus on the transverse vibration of a LCB with multiple concentrated masses representing a novel semi-analytical solution method for two different boundary conditions. Moreover, the influence of location and numbers of point mass on the natural frequencies as well as mode shapes are taken into account. Ultimately, interesting outcomes are outlined in conclusions.

2. Governing Equations of Motion

A general LCBs with multiple concentrated masses is considered as shown in Fig. 1. Some required initial assumptions are made as below:

The Euler-Bernoulli beam theory is used and the beam is subjected to clamp-free and simply-supported boundary conditions.

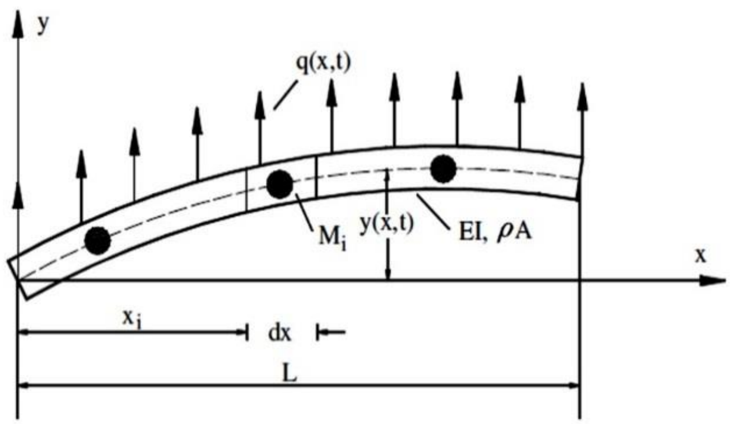

Fig. 1: A composite beam with multiple point masses

The relation between the bending and torsional moments with transverse displacement and rotation of the beam are represented as below [1]:

$$M = EIy'' - K\varphi'$$
$$T = -Ky'' + GJ\varphi' \qquad (1)$$

where EI is flexural rigidity, GJ is torsional rigidity and K represents bending-twisting coupling stiffness. It should be noticed that derivatives are considered with respect to x. These rigidities are defined in terms of components of flexural stiffness matrix as follows:

$$EI = D_{22} - \frac{{D_{12}}^2}{D_{11}},$$

$$K = 2\left(D_{26} - \frac{D_{12}D_{16}}{D_{11}}\right)$$

$$GJ = 4\left(D_{66} - \frac{{D_{16}}^2}{D_{11}}\right)$$

where

$$D_{ij} = \int_{-h/2}^{h/2} \bar{Q}_{ij} y^2 dy$$

in which h refers to the beam thickness and $\bar{Q}_{ij}$ is reduced stiffness matrix of laminated composites ($i, j = 1, 2\ and\ 6$).

In Fig. 1, the point mass M_i is assumed to be distributed along dx element, $\overline{m_i}$ is mass distribution and x_i shows the distance of M_i from the very beginning of the beam. Thus,

$$M_i = \overline{m_i} dx \tag{2}$$

The distributing function is represented via applying step function along the beam length, and the concentration is presented by delta Dirac function as follows:

$$m_i(x) = \overline{m_i}[u(x - x_i) - u(x - x_i - dx)] \tag{3}$$

$$\begin{aligned} \lim_{dx\to 0} m_i(x) &= \lim_{dx\to 0} \frac{M_i}{dx}[u(x - x_i) - u(x - x_i - dx)] \\ &= M_i \delta\,(x - x_i) \end{aligned} \tag{4}$$

Fig. 2 depicts the free body diagram of a beam element.

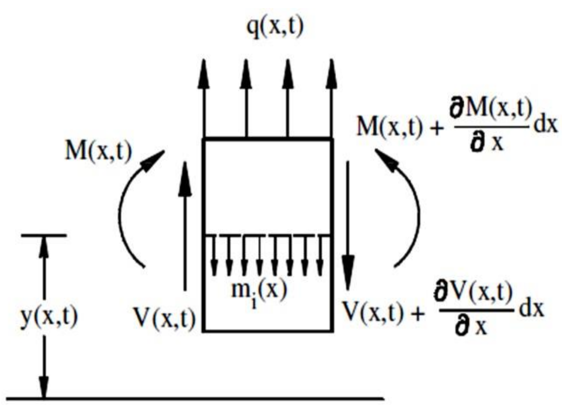

Fig. 2: Free body diagram of a beam element

in which $V(x, t)$ denotes shearing force and $M(x, t)$ is the bending moment. Using equilibrium equations, the following equations are obtained in terms of bending and torsional moments:

$$\begin{aligned} &\frac{\partial^2 M(x,t)}{\partial x^2} + \rho A\left[1 + \frac{M_i}{\rho A}\delta(x - x_i)\right]\frac{\partial^2 y(x,t)}{\partial t^2} = q(x,t) \\ &\frac{\partial T(x,t)}{\partial x} - I_\alpha \frac{\partial^2 \varphi(x,t)}{\partial t^2} = 0 \end{aligned} \tag{5}$$

where I_α is the polar mass moment of inertia per length.

In order to investigate transverse free vibration of the beam, external loading should be zero, i.e. $q(x, t) = 0$. Therefore, governing equations of motion for transverse free vibration of a beam with N point masses in terms of displacement and rotation can be written as:

$$EI\frac{\partial^4 y}{\partial x^4} - K\frac{\partial^3 \varphi}{\partial x^3} + \rho A\left[1 + \sum_{i=1}^{N}\frac{M_i}{\rho A}\delta(x - x_i)\right]\frac{\partial^2 y}{\partial t^2} = 0 \quad (6)$$

$$GJ\frac{\partial^2 \varphi}{\partial x^2} - K\frac{\partial^3 y}{\partial x^3} - I_\alpha\frac{\partial^2 \varphi}{\partial t^2} = 0 \quad (7)$$

3. Solution Method

The following harmonic solution could be applied for Eqs. (6) and (7) to separate the solution with respect to space and time:

$$y(x,t) = Y(x)e^{i\omega t}$$
$$\varphi(x,t) = \phi(x)e^{i\omega t} \quad (8)$$

Given the particular studied stacking sequences in this research (unidirectional and cross-ply laminated composites), one can rightly claim that the coupling parameter K equals to zero. Subsequently, substituting Eq. (7) into the (6) and using Eq. (8) yields:

$$EI\frac{d^4 Y}{dx^4} + \rho A\left[1 + \sum_{i=1}^{N}\frac{M_i}{\rho A}\delta(x - x_i)\right](-\omega^2)Y(x) = 0 \quad (9)$$

The dimensionless form of Eq. (9) can be rewritten as:

$$w^4(\zeta) - \lambda^4\left[1 + \sum_{i=1}^{N}\alpha_i\delta(\zeta - \zeta_i)\right]w(\zeta) = 0 \quad (10)$$

where $W = Y/L, \zeta = x/L, \alpha_i = M_i/\rho AL$ and

$$\lambda^4 = \rho AL^4\omega^2/EI \quad (11)$$

After simplification, Eq. (10) will be in the following form:

$$w^{iv}(\zeta) - \lambda^4 w(\zeta) = B(\zeta) \quad (12)$$

in which

$$B(\zeta) \triangleq \lambda^4\sum_{i=1}^{N}\alpha_i\delta(\zeta - \zeta_i)\, w(\zeta) \quad (13)$$

Accordingly, natural frequencies and the corresponding mode shapes can be found solving Eq. (12). It must be noticed that $w(\zeta)$ should be the same as the eigen-mode of uniform beam for region between two concentrated masses. The solution for overall beam can, therefore, be assumed as a combination of standard trigonometric and hyperbolic functions in which the coefficients of combination are generalized functions:

$$w(\zeta) = c_1 sin\,(\lambda\zeta) + c_2 cos\,(\lambda\zeta) + c_3 sinh\,(\lambda\zeta) + c_4 cosh\,(\lambda\zeta) \quad (14)$$

Assume $\overline{w}(\zeta)$ is a solution of a uniform beam without concentrated masses that satisfies the following equation:

$$\overline{w}(\zeta)^4 - \lambda^4 \overline{w}(\zeta) = 0 \qquad (15)$$

The first, second, third and fourth derivations of Eq. (14) with respect to x are:

$$\begin{aligned}
w'(\zeta) &= (\acute{c}_1 sin\lambda\zeta + \acute{c}_2 cos\lambda\zeta + \acute{c}_3 sinh\lambda\zeta + \acute{c}_4 cosh\lambda\zeta) + \overline{w}'(\zeta) \\
w'(\zeta) &= (\acute{c}_1 sin\lambda\zeta + \acute{c}_2 cos\lambda\zeta + \acute{c}_3 sinh\lambda\zeta + \acute{c}_4 cosh\lambda\zeta) + \overline{w}'(\zeta) \\
\mathrm{w}'''(\zeta) &= \lambda^2(-\mathrm{c}_1{}''' sin\lambda\zeta - \mathrm{c}_2{}''' cos\lambda\zeta + \mathrm{c}_3{}''' sinh\lambda\zeta + \mathrm{c}_4{}''' cosh\lambda\zeta) + \overline{\mathrm{w}}'''(\zeta) \\
\mathrm{w}^{iv}(\zeta) &= \lambda^3\left(-\mathrm{c}_1{}^{iv} sin\lambda\zeta + \mathrm{c}_2{}^{iv} cos\lambda\zeta + \mathrm{c}_3{}^{iv} sinh\lambda\zeta + \mathrm{c}_4{}^{iv} cosh\lambda\zeta\right) + \overline{\mathrm{w}}^{iv}(\zeta)
\end{aligned} \qquad (16)$$

The above equations can be represented in the matrix form as below:

$$\begin{bmatrix} sin\lambda\zeta & cos\lambda\zeta & sinh\lambda\zeta & cosh\lambda\zeta \\ cos\lambda\zeta & -sin\lambda\zeta & cosh\lambda\zeta & sinh\lambda\zeta \\ -sin\lambda\zeta & -cos\lambda\zeta & sinh\lambda\zeta & cosh\lambda\zeta \\ -cos\lambda\zeta & sin\lambda\zeta & cosh\lambda\zeta & sinh\lambda\zeta \end{bmatrix} \begin{bmatrix} \mathrm{c}'_1 \\ \mathrm{c}'_2 \\ \mathrm{c}'_3 \\ \mathrm{c}'_4 \end{bmatrix} = \begin{bmatrix} 0 \\ 0 \\ 0 \\ \frac{B(\zeta)}{\lambda^3} \end{bmatrix} \qquad (17)$$

Where

$$c_1{}' = \frac{-cos\lambda\zeta}{2\lambda^3} B(\zeta), \qquad c_3{}' = \frac{cosh\lambda\zeta}{2\lambda^3} B(\zeta)$$
$$c_2{}' = \frac{sin\lambda\zeta}{2\lambda^3} B(\zeta) \qquad c_4{}' = \frac{-sinh\lambda\zeta}{2\lambda^3} B(\zeta) \qquad (18)$$

Integration of Eqs. (18) results in:

$$\begin{aligned}
c_1 &= -\frac{\lambda}{2}\sum_{i=1}^{N} \alpha_i w(\zeta_i)\, cos(\lambda\zeta_i)\, u(\zeta - \zeta_i) + d_1 \\
c_2 &= \frac{\lambda}{2}\sum_{i=1}^{N} \alpha_i w(\zeta_i)\, sin(\lambda\zeta_i)\, u(\zeta - \zeta_i) + d_2 \\
c_3 &= \frac{\lambda}{2}\sum_{i=1}^{N} \alpha_i w(\zeta_i)\, cosh(\lambda\zeta_i)\, u(\zeta - \zeta_i) + d_3 \\
c_4 &= -\frac{\lambda}{2}\sum_{i=1}^{N} \alpha_i \mathrm{w}(\zeta_i)\, \mathrm{sinh}(\lambda\zeta_i)\, \mathrm{u}(\zeta - \zeta_i) + d_4
\end{aligned} \qquad (19)$$

where d_i $(i = 1,2,3\ and\ 4)$ are integration constants. Substituting Eqs. (19) into Eq. (14) gives the eigen-mode of the problem in a closed-form solution:

$$w(\zeta) = \lambda \sum_{i=1}^{N} \alpha_i w(\zeta_i) T(\zeta - \zeta_i)\, u(\zeta - \zeta_i) + D(\zeta) \tag{20}$$

where

$$D(\zeta) = d_1 sin\,(\lambda\zeta) + d_2 cos\,(\lambda\zeta) + d_3 sinh\,(\lambda\zeta) + d_4 cosh\,(\lambda\zeta)$$
$$T(\zeta) \triangleq \frac{1}{2}[sinh(\lambda\zeta) - sin(\lambda\zeta)] \tag{21}$$

in which $u(\zeta - \zeta_i)$ refers to unit step (Heaviside) function, which is the derivative of Dirac delta function, indicating a jump discontinuity at ζ_i. The α_i stands for dimensionless mass values evaluated at the concentrated mass sections ζ_i. The $w(\zeta_i)$ value at the mass point cross-section ζ_i can be selected by applying the distributional product with Dirac's delta to the bending deformation continuous function provided by in the some simplified form which we give consent to waiver for more explain them.

The solution of the eigen-mode governing equation (Eq. (13)) is given by Eqs. (20) and (21). Therefore, Eq. (20) can be updated as follows:

$$\begin{aligned} w(\zeta) = d_1 &\left[\lambda \sum_{i=1}^{j-1} \alpha_i \bar{\mu}_i T(\zeta - \zeta_i) u(\zeta - \zeta_i) + sin\,(\zeta)\right] \\ &+ d_2 \left[\lambda \sum_{i=1}^{j-1} \alpha_i \bar{\eta}_i T\big(\zeta_j - \zeta_i\big) u(\zeta - \zeta_i) + cos\,(\zeta)\right] \\ &+ d_3 \left[\lambda \sum_{i=1}^{j-1} \alpha_i \bar{\gamma}_i T\big(\zeta_j - \zeta_i\big)\, u(\zeta - \zeta_i) + sin\ h(\zeta)\right] \\ &+ d_4 \left[\lambda \sum_{i=1}^{j-1} \alpha_i \bar{\kappa}_i T\big(\zeta_j - \zeta_i\big) u(\zeta - \zeta_i) + cosh\,(\zeta)\right] \end{aligned} \tag{22}$$

The integration constants d_1, d_2, d_3 and d_4 can be easily evaluated by applying relevant boundary conditions. The first and second derivatives of the eigen-mode could be obtained by means of single and double differentiation of Eq. (14). Thus, the solution of the eigen-mode in terms of the basic functions in Eq. (22) would be:

$$
\begin{aligned}
w(\zeta) = e_1 &\left[\lambda \sum_{i=1}^{j-1} \alpha_i \mu_i g_4(\lambda\zeta - \lambda\zeta_i) u(\zeta - \zeta_i) + g_1(\lambda\zeta)\right] \\
&+ e_2 \left[\lambda \sum_{i=1}^{j-1} \alpha_i \eta_i g_4(\lambda\zeta - \lambda\zeta_i) u(\zeta - \zeta_i) + g_2(\lambda\zeta)\right] \\
&+ e_3 \left[\lambda \sum_{i=1}^{j-1} \alpha_i \gamma_i g_4(\lambda\zeta - \lambda\zeta_i)\, u(\zeta - \zeta_i) + g_3(\lambda\zeta)\right] \\
&+ e_4 \left[\lambda \sum_{i=1}^{j-1} \alpha_i \kappa_i g_4(\lambda\zeta - \lambda\zeta_i) u(\zeta - \zeta_i) + g_4(\lambda\zeta)\right]
\end{aligned} \tag{23}
$$

To obtain unknown coefficients in Eq. (23), specific boundary conditions should be applied. Two boundary conditions, i.e., SS (S stands for simply-supported boundary) and CF (C and F stand for clamped and free, respectively) are considered here. In the case of simply-supported boundary conditions, vertical displacements and moments are zero, i.e., $w(0) = w''(0) = w(1) = w''(1) = 0$, and consequently $e_1 = e_3 = 0$. In the case of clamped-free boundary conditions, vertical displacement and slope at clamped boundary are zero and moment and shear force are zero at free boundary, i.e., $w(0) = w'(0) = w''(1) = w'''(1) = 0$ and consequently $e_1 = e_2 = 0$ for boundary condition at $\zeta = 0$. The frequency equations are derived and numerically solved in order to obtain natural frequencies of the beams with multiple concentrated masses, and the corresponding explicit expressions of the vibration modes.

4. Results and Discussion

4.1. Validation

First, to verify outcomes of the proposed method being associated with free vibration of a composite beam with multiple point masses, the first four frequencies of a cantilever composite beam without point masses are provided from the Ref. [1]. Table. 1 compares natural frequencies of a cantilevered composite beam. It is seen that findings of present study are acceptably close to those of Ref. [1]. Therefore, it confirms the closed-form solution obtained for free vibration of LCBs.

Table 1. Comparison of first four frequencies (Hz) of a cantilever composite beam.

	ω_1	ω_2	ω_3	ω_4
Present study	8.040	50.39	141.0	275.9
Reference [1]	8.040	50.39	141.0	276.0
Difference, %	0	0	0	0.0004

Now, the frequency behavior of a circular composite shaft with [0/90/0/90]s lay-up and length of *L*=560 mm, inner radius of *r*=25 mm, total thickness of *t*=0.54 mm, mass moment of inertia of 3.4×10-4 kg.m2 is investigated. Also, the material properties of this orthotropic beam are $E_{11} = 155.8\,GPa$, $E_{22} = 10.36\,GPa$, $G_{12} = 6.67\,GPa$ and $\upsilon_{12} = 0.28$. The first four frequencies of this shaft are reported in Table. 2 for both SS and CF boundary conditions. The ω_{0i} (i=1-4) indicates natural frequencies of a beam without point mass. Table. 2 shows that the natural frequencies of a simply-supported beam are higher than those of a cantilever beam.

Table 2. First four natural frequencies (Hz) of a cross-ply circular composite shaft with different boundary conditions.

Boundary condition	ω_{01}	ω_{02}	ω_{03}	ω_{04}
SS	57.76	81.68	100.04	115.52
CF	44.62	70.60	91.33	108.06

4.2. The Effect of Amount and Location of Point Mass

To study the effect of point mass values and locations, three different values and locations are considered. Results of natural frequencies for SS and CF boundary conditions are presented in Table. 3 and Table 4, respectively. In these tables, α_i indicates the ratio of point mass to total mass of the beam and ζ_i indicates the ratio of the mass location to the beam's length. The results indicate that dimensionless natural frequencies decrease in the presence of point masses and all of the frequency ratios in Tables. 3 and .4 are less than 1. Natural frequencies of a simply-supported beam with masses at locations of $\zeta = 0.25$ and 0.75 are the same due to symmetric boundary conditions. If the mass gets closer to the center of the beam, the more reduction in dimensionless frequencies is observed. This phenomenon also happens for a cantilever beam while the mass gets closer to the free end of the beam.

Table 3. Frequency ratios of a simply-supported cross-ply beam with different values and locations of point mass

SS	ζ=0.25			ζ=0.5			ζ=0.75		
	α=0.1	α=1	α=10	α=0.1	α=1	α=10	α=0.1	α=1	α=10
ω_1/ω_{01}	0.988003	0.912773	0.730693	0.977417	0.870973	0.682345	0.988003	0.912773	0.730693
ω_2/ω_{02}	0.979027	0.916995	0.884363	1	1	1	0.979027	0.916995	0.884363
ω_3/ω_{03}	0.990923	0.974536	0.969196	0.980433	0.935004	0.915694	0.990923	0.974536	0.969196
ω_4/ω_{04}	1	1	0.999986	1	0.999999	0.999998	1	1	0.999986

Table 4. Frequency ratios of a clamped-free (CF) cross-ply beam with different values and locations of point mass.

CF	ζ=0.25			ζ=0.5			ζ=0.75		
	α=0.1	α=1	α=10	α=0.1	α=1	α=10	α=0.1	α=1	α=10
ω_1/ω_{01}	0.999527	0.995245	0.953498	0.994352	0.952266	0.798284	0.980234	0.881798	0.694954
ω_2/ω_{02}	0.991354	0.927257	0.773509	0.977895	0.896377	0.831062	0.999211	0.996442	0.99453
ω_3/ω_{03}	0.976956	0.90465	0.871575	0.999984	0.999935	0.999905	0.985907	0.946414	0.926823
ω_4/ω_{04}	0.9836	0.958848	0.952379	0.981063	0.942219	0.927851	0.986312	0.963878	0.957335

4.3. The Effect of Point Masses Number

In this section, the effect of point masses number on the natural frequencies of a composite beam is investigated. For this purpose, different numbers of masses 1, 2, 3, 5, 7, 10 in symmetric locations of beam length have been studied and the frequency equation in terms of dimensionless mass αi is plotted in Fig. 3 and .4 for SS and CF boundary conditions, respectively.

Figs. 3 and .4 clarify that frequency ratio decreases in presence of the point masses on the beam regardless of the numbers of masses. Also, frequency ratio is more affected by increasing the number of masses due to increasing of total system mass. Comparing Figs. 3 and 4., it is also found that the differences between frequency ratio curves are more significant in a cantilever beam than a simply-supported one. This phenomena is related to symmetric of boundary condition in the simply supported beam. These results can practically be used for designing of different composite shafts with multiple concentrated masses.

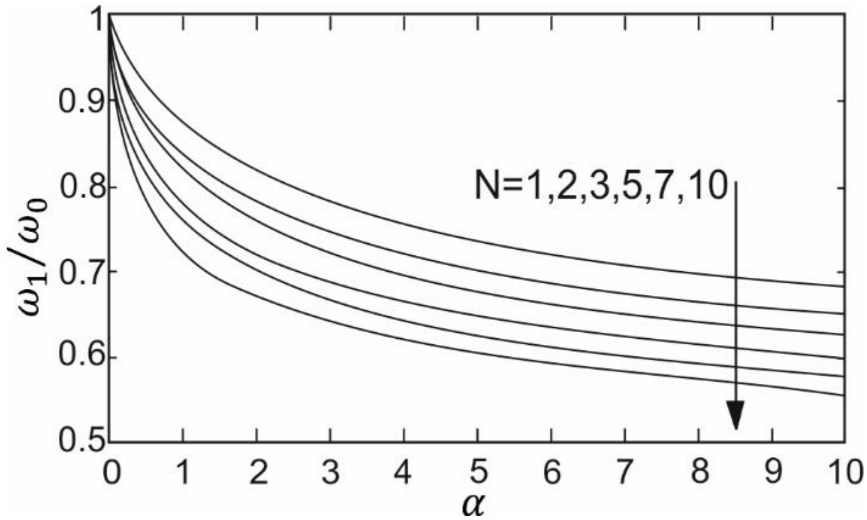

Fig. 3: The effect of number of point masses on the frequency ratio of a simply-supported composite beam

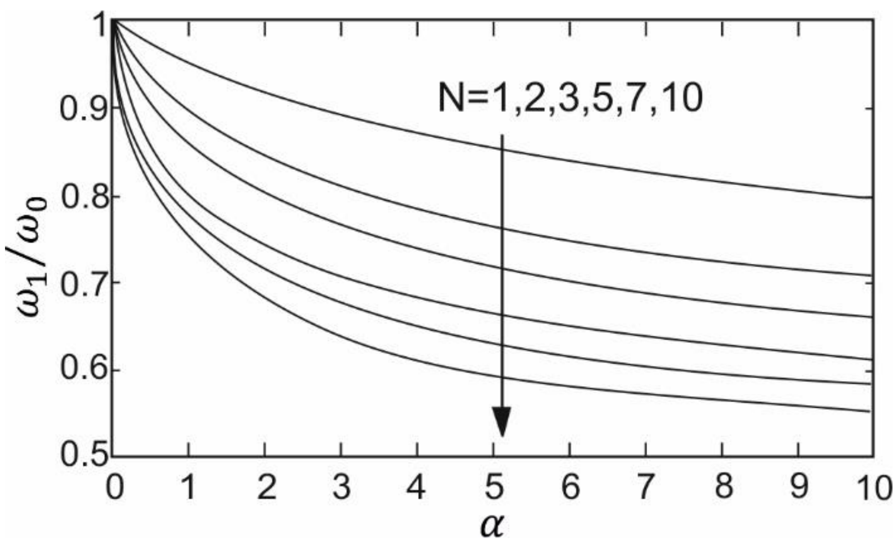

Fig. 4: The effect of number of point masses on the frequency ratio of a cantilever composite beam

5. Conclusions and Outlooks

Vibration response of equipment installed on the beam and shafts is of great interest for design engineers in various industries. In this study, free vibration of a LCB with multiple concentrated masses along the beam length is solved for the first time. More explicitly, the effects associated with value, location and number of point masses on the natural frequencies and mode shapes of a composite beam with simply-supported (SS) and cantilever-free (CF) boundary conditions are investigated in detail. Results suggested that natural frequencies of a simply-supported beam are more than those of a cantilever beam. It was seen that increasing the value of point masses results in decrease of natural frequencies. In simply-supported boundary conditions, the most reduction in vibration amplitude happens at the center of composite beam. In a cantilever beam, nevertheless, the most significant reduction in frequency occurs when a point mass is located at the free end.

Nomenclature

T	: Torsion moment	x	: Location
M	: Bending moment	η	: Dimensionless location
EI	: Bending stiffness rigidity	D	: Dimensionless differential operator
GJ	: Torsional rigidity	$\bar{g}_i$	: General basic functions
k	: Coupling stiffness	g_i	: Basic geometry coordinate functions
D_{ij}	: Bending stiffness matrix	W	: Displacement
m	: Beam mass	q	: Cross force on beam's unite length
I_α	: Mass moment of inertia	α_i	: Concentrated mass on beam's mass ratio
y	: Transverse displacement	ζ_i	: Mass location on beam length ratio
φ	: Torsion angle	m_i	: Point mass distribution
y''	: Second derivative of displacement	δ	: Dirac delta function
φ'	: First derivative of torsion angle	ρ	: Beam density
t	: Time	A_i	: Arrays of general basic functions
L	: Beam length	ω	: Natural frequency
$u(\zeta-\zeta_i)$	: Heaviside step function		

Conflict of Interest Statement

The author(s) declared no potential conflicts of interest with respect to the research, authorship, and/or publication of this article.

Funding

The author(s) received no financial support for the research, authorship, and/or publication of this article.

ORCID ID

Ahmad Reza Ghasemi https://orcid.org/0000-0002-9326-4990

References

1. Banerjee, J. R. (2001). Explicit analytical expressions for frequency equation and mode shapes of composite beams. *International Journal of Solids and Structures*, *38*(14), 2415-2426.
2. Ghayesh, M. H., Kazemirad, S., Darabi, M. A., & Woo, P. (2012). Thermo-mechanical nonlinear vibration analysis of a spring-mass-beam system. *Archive of Applied Mechanics*, *82*(3), 317-331.
3. Yang, C., & Oyadiji, S. O. (2016). Detection of delamination in composite beams using frequency deviations due to concentrated mass loading. *Composite Structures*, *146*, 1-13.
4. Khorshidi, K., Karimi, M., & Amabili, M. (2020). Aeroelastic analysis of rectangular plates coupled to sloshing fluid. *Acta Mechanica*, *231*, 3183-3198.
5. Karimi, M., Khorshidi, K., Dimitri, R., & Tornabene, F. (2020). Size-dependent hydroelastic vibration of FG microplates partially in contact with a fluid. *Composite Structures*, *244*, 112320.
6. Ghaheri, A., Keshmiri, A., & Taheri-Behrooz, F. (2014). Buckling and vibration of symmetrically laminated composite elliptical plates on an elastic foundation subjected to uniform in-plane force. *Journal of Engineering Mechanics*, *140*(7), 04014049.
7. Afsharmanesh, B., Ghaheri, A., & Taheri-Behrooz, F. (2014). Buckling and vibration of laminated composite circular plate on winkler-type foundation. *Steel and Composite Structures*, *17*(1), 1-19.
8. Mohandes, M., & Ghasemi, A. R. (2019). Discrepancies between free vibration of FML and composite cylindrical shells reinforced by CNTs. *Mechanics of Advanced Composite Structures*, *6*(2), 105-115.
9. Ghasemi, A. R., Taheri-Behrooz, F., Farahani, S. M. N., & Mohandes, M. (2016). Nonlinear free vibration of an Euler-Bernoulli composite beam undergoing finite strain subjected to different boundary conditions. *Journal of Vibration and Control*, *22*(3), 799-811.
10. Mohandes, M., & Ghasemi, A. R. (2016). Finite strain analysis of nonlinear vibrations of symmetric laminated composite Timoshenko beams using generalized differential

quadrature method. *Journal of Vibration and Control*, *22*(4), 940-954.

11. Ghasemi, A. R., & Mohandes, M. (2017). Nonlinear free vibration of laminated composite Euler-Bernoulli beams based on finite strain using generalized differential quadrature method. *Mechanics of Advanced Materials and Structures*, *24*(11), 917-923.
12. Nikolić, A. (2017). Free vibration analysis of a non-uniform axially functionally graded cantilever beam with a tip body. *Archive of Applied Mechanics*, *87*(7), 1227-1241.
13. Chaubey, A. K., Kumar, A., & Chakrabarti, A. (2018). Vibration of laminated composite shells with cutouts and concentrated mass. *AIAA Journal*, *56*(4), 1662-1678.
14. Fang, X., Chuang, K. C., Yuan, Z. W., & Huang, Z. L. (2018). Defect mode-induced unidirectional flexural wave transmission using prismatic beams with concentrated gradient masses. *Journal of Applied Physics*, *123*(22), 224901.
15. Kubojima, Y., Sonoda, S., & Kato, H. (2018). Practical techniques for the vibration method with additional mass: bending vibration generated by tapping cross section. *Journal of wood science*, *64*(1), 16-22.
16. Amoozgar, M. R., Shaw, A. D., Zhang, J., & Friswell, M. I. (2019). Composite blade twist modification by using a moving mass and stiffness tailoring. *AIAA Journal*, *57*(10), 4218-4225.
17. Dilena, M., Dell'Oste, M. F., Fernández-Sáez, J., Morassi, A., & Zaera, R. (2019). Mass detection in nanobeams from bending resonant frequency shifts. *Mechanical Systems and Signal Processing*, *116*, 261-276.
18. Eken, S., Cihan, M., & Kaya, M. O. (2020). Vibration and stability analysis of a spinning thin-walled composite beam carrying a rigid body. *Archive of Applied Mechanics*, 1-14.